

# Clustered DNA double-strand break formation and the repair pathway following heavy-ion irradiation

Yoshihiko Hagiwara<sup>1,†</sup>, Takahiro Oike<sup>1,†</sup>, Atsuko Niimi<sup>2,†</sup>,  
Motohiro Yamauchi<sup>3</sup>, Hiro Sato<sup>1</sup>, Siripan Limsirichaikul<sup>4</sup>, Kathryn D. Held<sup>5,6</sup>,  
Takashi Nakano<sup>1,2</sup> and Atsushi Shibata<sup>7,\*</sup>

<sup>1</sup>Department of Radiation Oncology, Gunma University, 3-39-22, Showa-machi, Maebashi, Gunma, 371-8511, Japan

<sup>2</sup>Research Program for Heavy Ion Therapy, Division of Integrated Oncology Research, Gunma University Initiative for Advanced Research (GIAR), Maebashi, Gunma, 371-8511, Japan

<sup>3</sup>Department of Radiation Biology and Protection, Atomic Bomb Disease Institute, Nagasaki University, Nagasaki, 852-8523, Japan

<sup>4</sup>Faculty of Pharmacy, Silpakorn University, Nakhon Pathom, 73000, Thailand

<sup>5</sup>Department of Radiation Oncology, Massachusetts General Hospital/Harvard Medical School, Boston, MA 02114, USA

<sup>6</sup>International Open Laboratory, Gunma University Initiative for Advanced Research (GIAR), Maebashi, Gunma, 371-8511, Japan

<sup>7</sup>Education and Research Support Center (ERSC), Graduate School of Medicine, Gunma University, 3-39-22, Showa-machi, Maebashi, Gunma, 371-8511, Japan

\*Corresponding author. Education and Research Support Center, Graduate School of Medicine, Gunma University, 3-39-22, Showa-machi, Maebashi, Gunma, 371-8511, Japan. Tel: +81-27-220-7977; Fax: +81-27-220-7909; Email: shibata.at@gunma-u.ac.jp

<sup>†</sup>These authors contributed equally to this work.

(Received 15 August 2018; revised 4 October 2018; editorial decision 8 October 2018)

## ABSTRACT

Photons, such as X- or  $\gamma$ -rays, induce DNA damage (distributed throughout the nucleus) as a result of low-density energy deposition. In contrast, particle irradiation with high linear energy transfer (LET) deposits high-density energy along the particle track. High-LET heavy-ion irradiation generates a greater number and more complex critical chromosomal aberrations, such as dicentric and translocations, compared with X-ray or  $\gamma$  irradiation. In addition, the formation of >1000 bp deletions, which is rarely observed after X-ray irradiation, has been identified following high-LET heavy-ion irradiation. Previously, these chromosomal aberrations have been thought to be the result of misrepair of complex DNA lesions, defined as DNA damage through DNA double-strand breaks (DSBs) and single-strand breaks as well as base damage within 1–2 helical turns (<3–4 nm). However, because the scale of complex DNA lesions is less than a few nanometers, the large-scale chromosomal aberrations at a micrometer level cannot be simply explained by complex DNA lesions. Recently, we have demonstrated the existence of clustered DSBs along the particle track through the use of super-resolution microscopy. Furthermore, we have visualized high-level and frequent formation of DSBs at the chromosomal boundary following high-LET heavy-ion irradiation. In this review, we summarize the latest findings regarding the hallmarks of DNA damage structure and the repair pathway following heavy-ion irradiation. Furthermore, we discuss the mechanism through which high-LET heavy-ion irradiation may induce dicentric, translocations and large deletions.

**Keywords:** heavy-ion irradiation; DNA double-strand breaks; super-resolution microscopy; DSB repair pathway; cancer treatment; radiotherapy

## INTRODUCTION

Ionizing radiation (IR) leads to genomic instability, which induces several cellular toxicity events: e.g. cell death, tumorigenesis, or

cellular senescence. In terms of genomic stability, photon and particle radiation with high linear energy transfer (LET) exhibits a variety of signatures of chromosomal aberrations [1]. The effects of

IR-dependent DNA damage on human health has been studied, particularly the effects on astronauts during periods of space travel or on workers and the general public when radiation accidents occur [2]. In fact, because particle irradiation deposits high-density energy along the particle track, the dose to a cell with a single track traversal becomes the equivalent of a high dose of X-rays, even though the overall dose may be low. Despite the fact that the dose of IR is generally low in such circumstances, the health risks following high LET irradiation cannot be underestimated because high LET irradiation densely deposits high energy, such a concentrated high-energy deposition can induce a significant level of DNA damage and occasionally can also generate DNA damage that may be unreparable or difficult to repair correctly. IR is used for cancer treatment in the form of radiotherapy [3]. In conventional radiotherapy, X-ray or  $\gamma$ -irradiation is used; however, because much of the X-ray or  $\gamma$ -irradiation energy is deposited in normal tissues before reaching tumors, a sufficient radiation dose may not be deliverable to the tumor with single-field irradiation. Recently, the efficacy of X-ray or  $\gamma$ -irradiation therapy has been improved through the use of advanced technology, such as intensity-modulated radiation therapy, which delivers radiation more precisely to tumors by controlling the direction and energy of radiation [4]. As a further advance in radiotherapy, particle radiation has been developed for cancer treatment. Particle therapy is promising because it has two great advantages compared with photon therapies [5]. First, carbon ion irradiation, which is categorized as a heavy-ion irradiation, shows a 2–3-fold greater relative biological effectiveness in killing cells than X-ray or  $\gamma$ -irradiation. In addition, heavy-ion radiation produces a highly concentrated dose distribution as a result of the Bragg peak effect, and this is significantly advantageous in that it can be used to intensively target cancer cells, while minimizing cellular damage to the surrounding normal tissues. However, despite the significant therapeutic benefits of particle therapy, the reasons underlying the higher efficacy of high-LET radiation for killing cancerous cells compared with that of photons remains poorly elucidated.

IR generates multiple types of DNA damage, including DNA double-strand breaks (DSBs), single-strand breaks (SSBs), base damage and DNA-protein cross links [1, 2, 6]. Of these, DSBs are considered critical DNA lesions that affect cellular fate because they lead to cell death or carcinogenesis when unrepaired or misrepaired [7]. In this review, we summarize recent findings obtained through advanced microscopy and molecular biology techniques and discuss the mechanisms underlying the severe chromosomal rearrangements, including dicentrics, translocations and large deletions, induced by high-LET heavy-ion irradiation in the context of DNA damage structure and its repair pathway. The elucidation of the mechanisms underlying chromosomal rearrangements following heavy-ion irradiation will be of significance in promoting precision radiotherapy through the consideration of gene status and DNA repair activity in tumors.

#### CLUSTERED DSB FORMATION AFTER HIGH-LET HEAVY-ION IRRADIATION

Accumulating evidence has demonstrated that heavy-ion irradiation causes a great number of dynamic chromosomal aberrations,

including chromosomal rearrangements, such as chromosome breaks, dicentrics, translocations and deletion mutations, compared with X-ray or  $\gamma$ -irradiation [1]. In addition, mutation analysis using transgenic mice that were developed to examine the mutation frequency at specific loci *in vivo* revealed that carbon ion irradiation significantly increased deletion mutation frequency in the liver, spleen and kidney [8, 9]. Significantly, DNA sequencing analysis revealed that carbon ion irradiation generated deletions of more than 1000 base pairs (bp), whereas  $\gamma$ -irradiation mainly induced deletions of <100 bp [9]. According to Monte Carlo simulations, it has been suggested that heavy-ion irradiation causes complex DNA lesions, defined as DNA damage containing both DSBs and SSBs, as well as base damage, within 1–2 helical turns (<3–4 nm) (as a comparison, the scale of chromatin fiber is shown in Fig. 1) [10, 11]. This is also referred to as clustered DNA damage. We recently identified the formation of multiple DSBs in close proximity (~700 nm) along the particle track [12]. To clarify the difference, we refer to multiple DSBs as clustered DSBs, in contrast to complex DNA lesions. It has been thought that complex DNA lesions may delay the speed of overall DNA repair because complex DNA lesions likely disrupt the recruitment of DNA repair proteins for each type of DNA damage. In addition, such disruption of the DNA repair process may lead to mis-repair; occasionally, the lesions themselves may not be repairable. Thus, complex DNA lesions are the most representative hallmark of DNA damage induced by high-LET heavy-ion radiation; however, the mechanisms through which complex DNA lesions cause chromosomal rearrangements, particularly dicentrics, translocations or large deletions, has been extensively debated because the scale of complex DNA lesions is of the order of 10–30 bp, i.e. <10 nm, whereas the scale of chromosomal rearrangement is of the order of >1000 bp, i.e. >50–100 nm distance, to be compared with a chromatin fiber region of 30 nm  $\times$  60 nm  $\times$  60 nm (1.08  $\times$  10<sup>-4</sup>  $\mu$ m<sup>3</sup>), which contains four nucleosomes when one nucleosome and linker are compacted within a square 30 nm each side. To explain the discrepancy between complex DNA lesions (~30 bp) and chromosomal rearrangements (>1000 bp) in terms of the scale, the possibility of mis-rejoining of two DSBs between distinct loci must be considered. Chromosomal

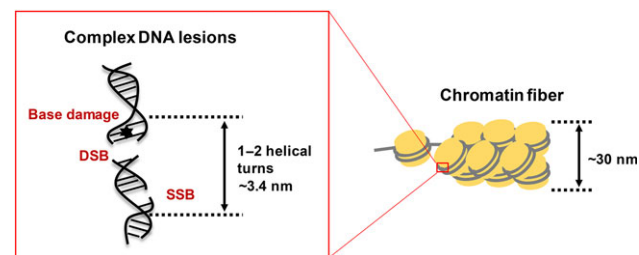


**Fig. 1. Scale diagrams of heavy-ion-induced DNA damage.** The scale diagrams of heavy-ion-induced complex DNA lesions and chromatin fiber. Heavy-ion radiation causes complex DNA lesions, which contain DSBs, and SSBs and/or base damage within 1–2 helical turns, along the particle track. The scale of a chromatin fiber is less than ~30 nm.

translocations are formed when two DSBs are mis-rejoined. Based on the ‘contact first’ model, which states that the joining of two broken chromosomes takes place when the breaks are located in a proximal position, if the clustered DSBs occur at the chromosome boundary, it will likely lead to interchromosomal exchange [13–15]. Similarly, when two DSBs are formed close to each other in the same chromosome, then intra-chromosomal exchange results in a deletion. Importantly, this notion is strongly supported by our finding of clustered DSB formation, which is detected by high- or super-resolution microscopy, after high-LET heavy-ion radiation. Previous reports identified that high-LET particle irradiation causes large phosphorylated H2AX ( $\gamma$ H2AX) foci, a marker of DSBs, along the particle track [16, 17]. In 2013, we reported, using high-resolution microscopy involving deconvolution in immunofluorescence samples, that  $\gamma$ H2AX foci encompass multiple smaller and closely localized foci, which we designate as clustered  $\gamma$ H2AX foci [18]. Significantly, such clustered IR-induced foci were identified in samples of a human tumor clinically treated with carbon ion radiotherapy; however, these clustered foci were not observed in a tumor treated with X-ray radiotherapy (in our study of human samples, we

examined 53BP1, another marker of DSBs, due to the high background of  $\gamma$ H2AX signals in human tumors) [19]. More recently, through super-resolution microscopy, we identified the formation of clustered (Replication Protein A) RPA foci, a marker of DSBs undergoing homologous recombination (HR), within  $\gamma$ H2AX signals in carbon ion-irradiated G2-phase cells (Fig. 2A–B) [12]. The average distance between two or three individual RPA foci within the  $\gamma$ H2AX signal was  $\sim$ 700 nm, although the distribution varied from 100 nm to 1500 nm (Fig. 2C) [12]. Similar to our findings, other groups showed that 2–3 RAD51 foci are closely localized within the 53BP1 signal after heavy-ion irradiation [20]. Taken together, these observations strongly suggest that multiple DSBs are generated in close proximity along the track of high-LET heavy-ion radiation. Importantly, we found a greater extent of RPA foci formation following high-LET carbon ion irradiation compared with that following low-LET irradiation [12]. To support the observations of the immunofluorescence microscopy work, Monte Carlo simulations suggested that several DSBs can be formed within 100 nm [11]. In addition, such clustered DSB formation was visualized by transmission electron microscopy using gold-labelled DNA-repair

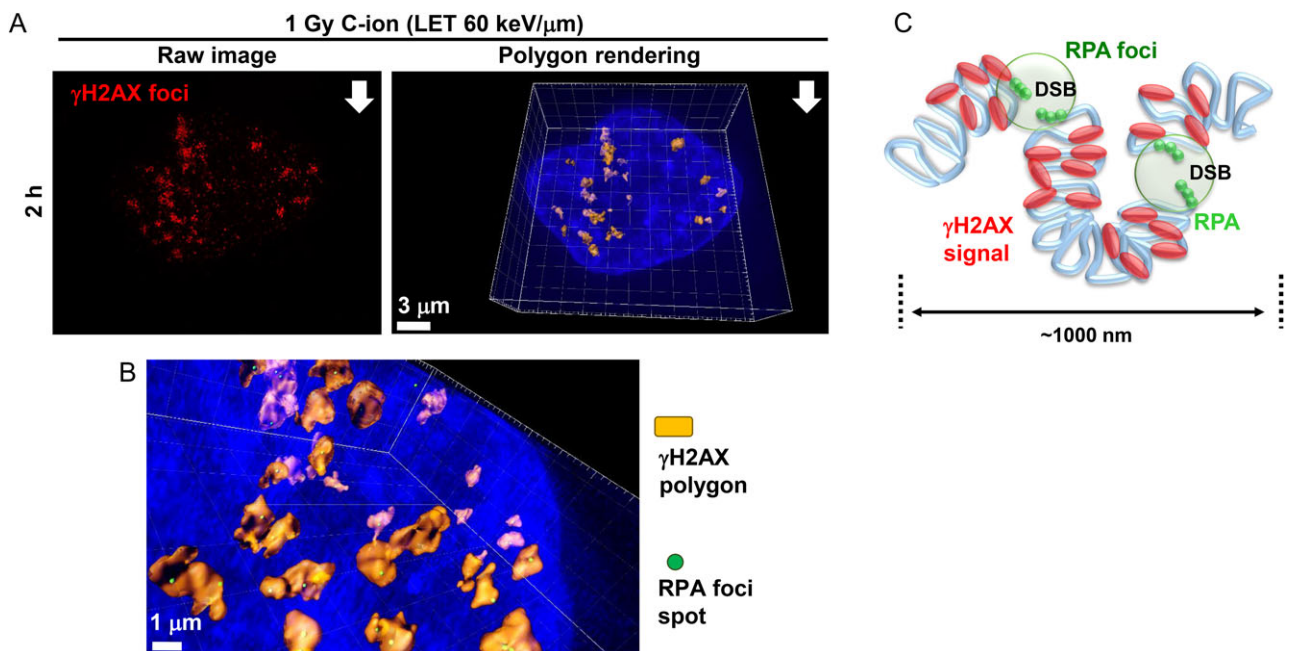


**Fig. 2.** 3D-SIM analysis reveals clustered DSB formation following heavy-ion irradiation. (A) Representative images for 3D  $\gamma$ H2AX polygon rendering using 3D-SIM analysis. 1BR hTERT cells were fixed at 2 h after 1 Gy carbon-ion irradiation (290 MeV/n, Mono, LET 60 keV/ $\mu$ m), and fixed cells were stained with antibodies for  $\gamma$ H2AX, RPA and CENPF and with DAPI. To detect RPA foci, which show clear and sharp signals for SIM analysis, G2 cells were examined. G2 cells were identified by CENPF (the original data are shown in [12]). The raw image of  $\gamma$ H2AX is shown in the left panel.  $\gamma$ H2AX polygon rendering, which is generated by surface mode in Imaris 8.1.2 (Bitplane, Zurich, Switzerland), is shown in the right panel.  $\gamma$ H2AX foci and DAPI are shown as yellow and blue polygons, respectively. The direction of the carbon ion radiation is indicated by a white arrow. (B) 3D polygon rendering of  $\gamma$ H2AX and the spot signal of RPA in (A) are shown. Clustered RPA foci are identified within the  $\gamma$ H2AX signal in carbon ion-irradiated G2 cells.  $\gamma$ H2AX the signal is shown by the polygon. RPA foci are shown as green spots. (C) A diagram for DSB distribution after high-LET particle irradiation. Super resolution imaging allows visualization of the distribution of  $\gamma$ H2AX along the chromatin loop. RPA forms a single focus representing a DSB unless  $>2$  DSBs are formed within 100 nm.

factors [21, 22]. However, we stress that the limitation of immunofluorescence microscopic analysis must be considered, as although super-resolution microscopy has excellent resolution (e.g. the 3D-SIM has a resolution of  $\sim 100$  nm in the  $x$ - and  $y$ -axes and a  $\sim 300$  nm resolution in the  $z$ -axis, and PALM and STORM have  $\sim 70$  nm resolution in the  $x$ - and  $y$ -axes), complex DNA lesions occurring within  $\sim 30$  nm cannot be identified by immunofluorescence microscopy [23]. In fact, we believe that the number of DSBs detected as RPA foci by 3D-SIM analysis is likely to be underestimated because the total number of RPA foci per cell following 1 Gy carbon ion (LET 60 keV/ $\mu$ m) irradiation in our study was smaller than that estimated by the simulations under similar conditions [11, 12]. Nevertheless, despite the limitation of the immunofluorescence study, the identification of clustered DSB formation is still important. Our study provided the notion that high-LET heavy-ion irradiation can cause clustered DSBs, which is a novel hallmark of heavy-ion-induced DSBs. We believe this is important because the formation of multiple DSBs on the scale of 100–1000 nm can increase the risk of inter- and intra-chromosomal exchange. As described above, the formation of multiple DSBs in the same chromosome or different chromosomes may result in dicentric or chromosomal translocations or large deletions. This idea is consistent with the observation that carbon ion irradiation generated deletions of  $>1000$  bp [9]. In the following section, we discuss in further detail the evidence showing that heavy-ion irradiation can cause DSBs at chromosome boundaries between two or more distinct chromosomes along the particle track.

#### FORMATION OF $\gamma$ H2AX FOCI AT THE CHROMOSOME BOUNDARY

X-rays or  $\gamma$ -irradiation, which are categorized as low LET, induce DSBs with a mostly random distribution in the nucleus. In contrast, heavy-ion irradiation deposits its energy densely along the track of the particle traversal. The formation of the particle track is clearly observed by  $\gamma$ H2AX staining when cells are irradiated horizontal to the beam direction [18]. The track becomes evident particularly when the particle has a high LET ( $>20$ – $40$  keV/ $\mu$ m). This feature is important when human cells are exposed to heavy-ion irradiation because human chromosomes occupy territories in the interphase nucleus. The territories form chromosome boundaries between each chromosome, although they are merged at the boundary between chromosomes [24, 25]. To date, two models have been proposed to explain the association of two DSB loci in the formation of rejoining-dependent translocations [15, 25, 26]. The contact first model proposes that rejoining of DSBs on distinct chromosomes can take place preferentially when the translocation partner loci are proximal. In the alternative ‘breakage first’ model, the persistent unrepaired DSBs roam the nuclear space in search of appropriate interaction partners, suggesting the requirement of large-scale motion in the nucleus. The former model is supported by evidence that chromosomal translocation between two close chromosomes is frequently observed in cancer specimens [27]. In addition, Yamauchi *et al.* demonstrated that pairing between IR-induced foci frequently occurs when the distance between the foci is  $<2$   $\mu$ m [28]. Thus, the region at the chromosome boundary is at risk of forming

chromosome rearrangements if multiple DSBs are generated in close proximity to it.

Through the use of immunofluorescence and fluorescence *in situ* hybridization, we showed that the frequency of  $\gamma$ H2AX foci at the chromosome boundary of chromosome 1 following carbon ion irradiation was  $>4$ -fold higher than that after X-ray irradiation (Fig. 3A) [29]. This observation is consistent with the idea that particle irradiation generates DSBs at the boundaries of two chromosomes along the track. As described in the previous section, our high- or super-resolution microscopy revealed that multiple DSBs are formed in close proximity following high-LET heavy-ion irradiation (Fig. 3B). By combining our imaging analysis and the evidence from previous chromosome and mutation analyses, we propose that multiple DSB formation within a limited area around chromosome boundaries is a crucial factor in the formation of chromosomal rearrangements and large deletions following high-LET heavy-ion irradiation (Fig. 3C).

#### DSB REPAIR PATHWAY FOLLOWING HEAVY-ION IRRADIATION

In human cells, DSBs are mainly repaired by either canonical non-homologous end joining (c-NHEJ) or HR [7]. In the past 10 years, studies have revealed that NHEJ functions throughout the cell cycle, whereas HR is active in the S/G2-phases following DNA replication. Recent studies have demonstrated that  $\sim 70\%$  of DSBs induced by X-rays or  $\gamma$ -irradiation are repaired by NHEJ in human cells, even in G2 phase (Fig. 4A) [30, 31]. Although the percentage of pathway usage between NHEJ and HR varies depending on the cell type, many studies suggest that NHEJ still largely contributes to DSB repair in S/G2. In contrast to X-rays or  $\gamma$ -irradiation, DSBs induced by high-LET heavy-ion irradiation are preferentially repaired by HR (Fig. 4B) [31, 32]. The greater HR dependency was suggested by a substantial DSB repair defect in BRCA2-defective human cells and Rad54-deficient mouse embryonic fibroblasts in the G2 phase [31]. However, there is some discrepancy regarding the high frequency of HR usage following high-LET heavy-ion irradiation because a LET-dependent increase in chromosomal aberrations was observed in G2 cells [33]. Since HR is an error-free repair pathway, if DSBs are precisely repaired by HR, chromosomal aberrations should not be observed. Thus, the chromosomal aberrations data suggest that some DSBs are likely repaired by error-prone repair pathways such as single-strand annealing (SSA) or alternative-NHEJ (alt-NHEJ) following excessive resection in G2 [34–36].

As an additional parameter leading to chromosomal aberrations following IR, the vulnerable G2/M checkpoint should be considered. In human cells, the G2/M checkpoint is turned on and arrests cell cycle progression when G2 cells contain  $>10$ – $20$   $\gamma$ H2AX foci; in other words, G2 cells with DSBs can progress into mitosis [37]. The duration of the G2/M checkpoint arrest becomes longer following high-LET heavy-ion irradiation compared with the duration following X-ray exposure when the same physical dose is used; however, irradiated cells are released from checkpoint arrest even after high-LET heavy-ion irradiation when the number of  $\gamma$ H2AX foci is  $<10$  (the number of  $\gamma$ H2AX foci after high-LET



heavy-ion irradiation is less than after X- or  $\gamma$ -ray irradiation, because such large  $\gamma$ H2AX foci must contain two or more DSBs) [18]. This incompleteness of the G2/M checkpoint arrest is thought to be one of the causes of chromosomal rearrangement by mis-segregation during mitosis, particularly after high-LET heavy-ion irradiation.

Similar to DSB repair in G2 cells, DSBs induced by high-LET heavy-ion irradiation increase the number of DSBs undergoing end

resection in G1 cells [38]. Following X-ray or  $\gamma$ -irradiation exposure, ~15% of DSBs undergo resection; however, since the length of resection is much shorter in G1 than that in G2 cells, the events are not detected as RPA foci [32]. In contrast, high-LET heavy-ion irradiation causes more active resection, which is detectable as RPA foci [32]. Although some resection is caused by high-LET heavy-ion irradiation, the HR pathway is still suppressed in the G1-phase to ensure that HR occurs only between sister chromatids. Therefore,

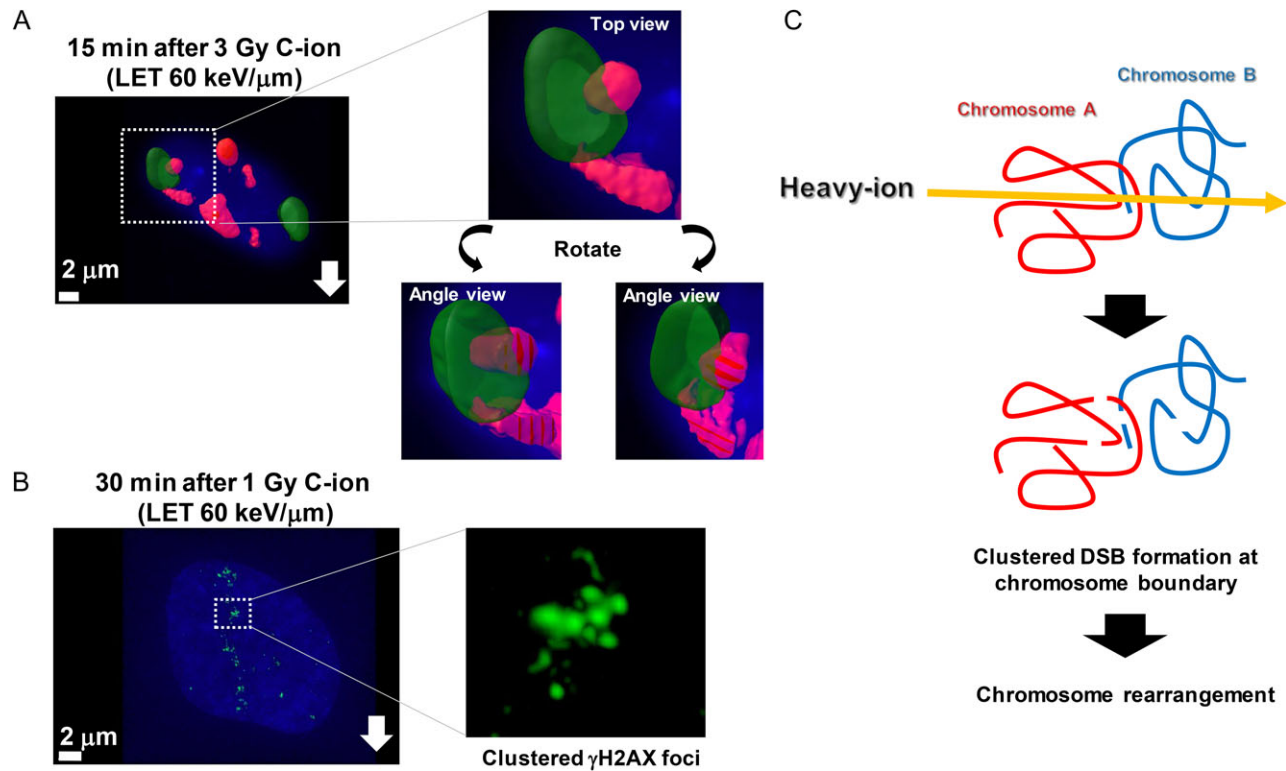


**Fig. 3.** Formation of clustered DSBs at the chromosome the boundary following heavy-ion irradiation. (A) The frequency of  $\gamma$ H2AX foci formation at chromosome boundary after high-LET carbon ion irradiation is greater than after X-rays. A representative image of  $\gamma$ H2AX and chromosome 1 using combination staining of immunofluorescence (IF) and fluorescence *in situ* hybridization (FISH) is shown. 1BR hTERT G1 cells were synchronized by contact inhibition. Cells were fixed at 15 min after 3 Gy carbon-ion irradiation (290 MeV/n, Mono, LET 70 keV/ $\mu$ m).  $\gamma$ H2AX foci, chromosome 1 and DAPI are shown by red, green and blue, respectively. Enlarged images are shown in the right panel. Images from different angles are shown in the right bottom panel. The percentage of  $\gamma$ H2AX foci formation at the chromosome boundary after carbon ion irradiation (8.64%) is 4-fold greater than that after X-rays (2.23%) [29]. The direction of the carbon ion radiation is indicated by a white arrow. (B) The representative image of clustered  $\gamma$ H2AX foci formation following carbon ion irradiation. Clustered  $\gamma$ H2AX foci in 1BR hTERT cells are also observed by high-resolution microscopy involving deconvolution, not 3D-SIM [18]. Cells were stained with  $\gamma$ H2AX and DAPI at 30 min after 1 Gy carbon-ion irradiation (290 MeV/n, Mono, LET 60 keV/ $\mu$ m). Enlarged  $\gamma$ H2AX foci are shown in the right panel.  $\gamma$ H2AX foci and DAPI are shown by green and blue. Although it is technically not feasible to obtain high-resolution or super-resolution Grade IF samples after sample preparation for FISH, combining evidence strongly suggests that  $\gamma$ H2AX foci formation at the chromosome boundary after high-LET carbon ion irradiation contains multiple DSBs. The direction of the carbon ion radiation is indicated by a white arrow. (C) A diagram of the formation of chromosome rearrangement via mis-rejoining between two distinct chromosomes following high-LET heavy-ion irradiation. High-LET heavy-ion radiation causes multiple DSB formation within a limited area. Furthermore, high-LET heavy-ion radiation can cause multiple DSBs at chromosome boundaries. If two or more DSBs are induced at the chromosome boundary between different chromosomes A and B, interchromosomal exchanges such as dicentrics or translocations may occur.

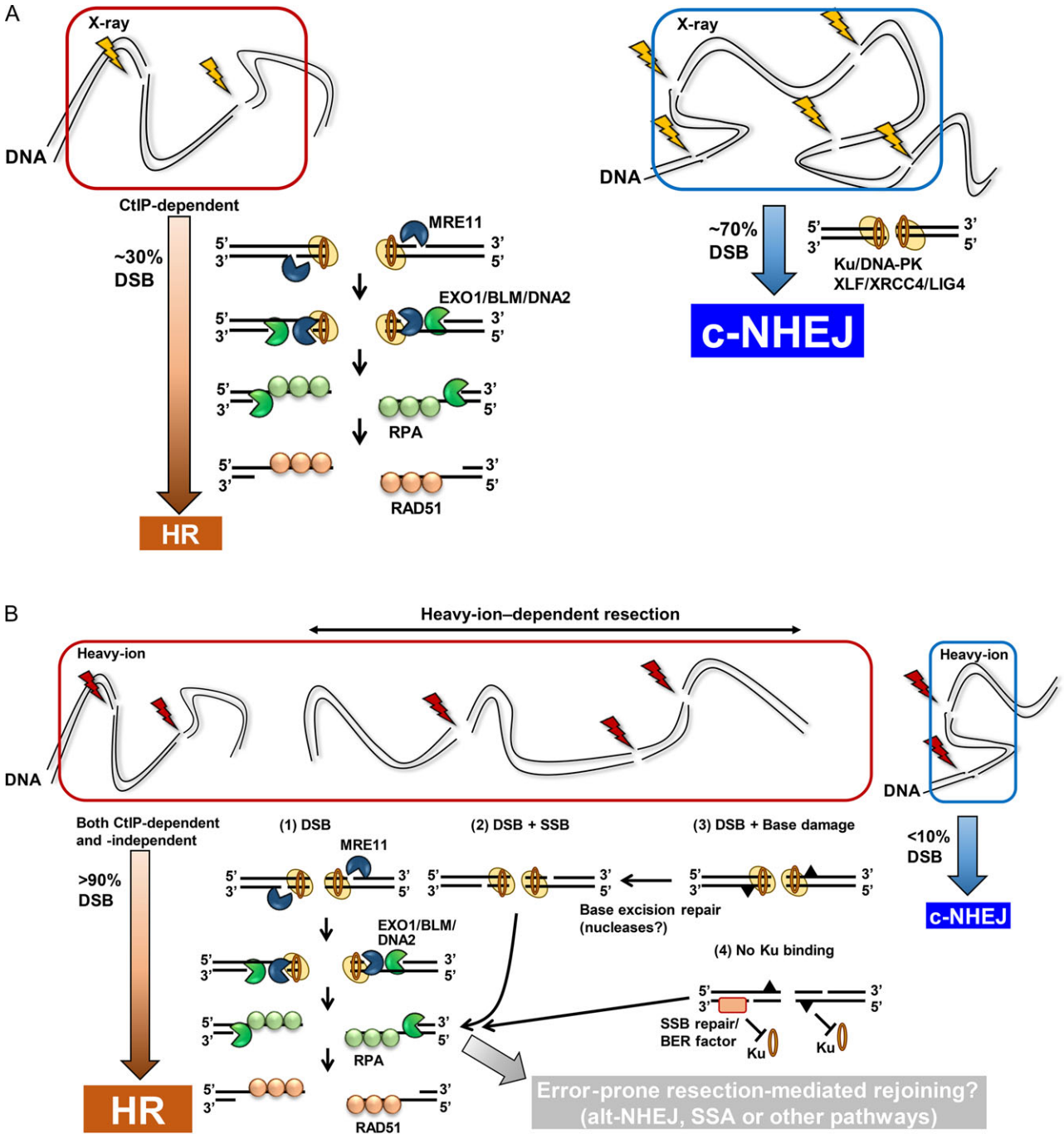


Fig. 4. DSB repair pathway following heavy-ion radiation. (A) The model of the DSB repair pathway in G2 cells following X-ray irradiation. Recent studies have demonstrated that ~70% of DSBs are repaired by NHEJ in human G2 cells, whereas ~30% of DSBs are repaired by HR in G2 cells. Ku70/80 and DNA-PKcs complex bind all the DSB ends. Approximately 70% of DSBs are rapidly rejoined using XLF, XRCC4 and LIG4 in c-NHEJ. For HR, DNA end resection is initiated by MRE11 endonuclease, which is stimulated by CtIP. MRE11 endonuclease activity creates nicks, followed by exonucleases digesting ssDNA either 3' to 5' or 5' to 3'. MRE11 digests ssDNA by its 3' to 5' exonuclease activity, proceeding to the DSB terminal, whereas EXO1 exonuclease digests ssDNA from 5' to 3' with BLM and DNA2. Extension of resection is promoted by BRCA1. The process of this pathway is summarized in [53]. Following resection, ssDNA is rapidly coated with RPA, which is then displaced by RAD51. RAD51 promotes recombination with the sister chromatid, and HR is completed. (B) The model of the DSB repair pathway following heavy-ion irradiation. Approximately 90% of DSBs induced by high-LET heavy-ion irradiation

DSBs undergoing resection in G1 cells are repaired by the non-HR pathway [39]. Nevertheless, importantly, since a DNA-PKcs inhibitor strongly blocks DSB repair in irradiated G1 cells following high-LET heavy-ion irradiation, and a poly (ADP-ribosyl) polymerase (PARP) inhibitor elicits a modest DSB repair defect, the c-NHEJ pathway seems to be the major pathway for repairing DSBs following high-LET heavy-ion irradiation (Fig. 5) [39]. Further analysis will be required in order to precisely understand the molecular mechanism underlying the DSB repair pathway following high-LET heavy-ion irradiation.

### TRANSLATIONAL RESEARCH IN HEAVY-ION THERAPY IN THE CONTEXT OF THE IDENTIFICATION OF DNA DAMAGE STRUCTURE AND THE REPAIR PATHWAY

Heavy ions have been used in cancer therapy for decades [3]. Carbon ions are most widely used for heavy-ion radiotherapy. Clinical studies have shown that carbon ion radiotherapy is effective for tumors resistant to conventional X-ray radiotherapy, e.g. pancreatic cancer and osteosarcoma [5, 40, 41]. Pre-clinical data suggest that the strong cell-killing effect of carbon ions is based on the ability of carbon ions to induce unreparable DSBs and/or lethal chromosomal aberrations. Consistent with the observations in *in vitro* studies, we identified the formation of clustered DSBs in a human tumor treated with carbon ion radiotherapy, but not in a tumor treated with X-ray radiotherapy, which provides a proof-of-principle for the superiority of carbon ions over X-rays in terms of clinical anti-tumor efficacy [19]. Importantly, carbon ion radiotherapy utilizes mixed-LET beams for the anatomically optimal delivery of radiation to a defined tumor target. This can lead to both intra- and inter-tumor heterogeneity in LET. Given that LET of carbon ions relates to anti-tumor efficacy via the formation of clustered DSBs, research into the assessment and management of LET heterogeneity in treatment planning of carbon ion radiotherapy will improve treatment efficacy. This aspect may be worth pursuing, especially in the context of tumor hypoxia, because previous studies have shown that DSBs induced by high-LET heavy ions are

preferentially repaired by HR and that HR efficacy is mitigated under hypoxia [42].

The next question concerns how cells progress to cell death or persistent growth arrest after high-LET heavy-ion irradiation. One possibility is that unreparable DSBs persist in irradiated G1 cells, undergoing apoptosis without going through mitosis or resulting in persistent growth arrest, e.g. senescence-like growth arrest (SLGA), because the G1/S checkpoint is highly sensitive and more efficiently limits genomic instability compared with the G2/M checkpoint unless ATM or p53 signaling is normal [43]. However, since ATM or p53-dependent DNA damage signaling is unlikely to be perfect in cancer cells, irradiated cells can progress into S/G2 cell cycle phases. The other possibility is that lethal chromosomal aberrations lead to cell death or mis-segregation during mitosis. As described above, clustered DSBs must be formed at the boundaries of two chromosomes along the particle track in cancer cells after radiotherapy. Chromosomal rearrangements in cancer cells are likely the cause of cell death during the first stage of mitosis or immediately after mitosis, which can prevent the survival of daughter cells, as observed in cells following X-ray or  $\gamma$ -irradiation exposure. Thus, such clustered DSBs can effectively prevent cancer cell growth by cell-killing effects in the first mitosis or at least before second mitosis, i.e. before generating daughter cells (Fig. 6).

### CONCLUSIONS AND REMAINING QUESTIONS

Advanced technologies, particularly immunofluorescence microscopy, have uncovered the three-dimensional structures of DSBs following heavy-ion irradiation. In addition, studies using molecular biology techniques have revealed in detail the mechanisms underlying DSB repair and the pathways used following heavy-ion irradiation. However, despite the novel findings in terms of DNA damage structure and the repair pathways, the repair events at the scale of <100 nm and cellular fate after high-LET particle irradiation are still unclear.

Although complex lesions have not been visualized, the complexity at DSB ends can be a critical factor affecting repair pathway, because it increases the number of DSBs undergoing resection. The

---

are repaired by resection-mediated pathway, i.e. mainly HR and others, e.g. SSA or alt-NHEJ. The increased percentage of HR usage after high-LET heavy-ion irradiation can be explained by the speed of DSB repair. In human G1 cells, which primarily use NHEJ but not other pathways, DSB repair after high-LET particle irradiation shows significantly slower kinetics than that after X- or  $\gamma$ -ray irradiation [31]. This suggests that DSB end complexity influences the speed of DSB repair. The current model proposes that, in G2 phase, NHEJ factor initially binds to DSB ends; however, when rapid NHEJ does not ensue, DSB end resection and HR occur [31, 45]. Thus, when DSB end complexity is induced by high-LET particle irradiation, as shown in (2) and (3), these DSBs showing the delay of DSB repair are repaired by HR. At DSB ends induced by high-LET particle irradiation, the resection is both CtIP-dependent and -independent. We postulate four pathways leading to resection-mediated DSB repair in heavy-ion dependent resection. (1) MRE11 endonuclease initiates resection with CtIP. After the incision, EXO1/BLM/DNA2 promote extension of resection as described above. (2) When SSBs are generated close to DSBs, it may bypass the step of MRE11/CtIP-dependent resection. (3) When base damage is generated close to DSBs, the damaged base is removed by DNA glycosylases and a nick is generated by AP endonucleases. Afterwards, the generated nick may trigger EXO1/BLM/DNA2-dependent extension of resection without MRE11/CtIP-dependent endonuclease activity. (4) Ku binding on the DSB end may be prevented by base damage or SSB repair or BER proteins in the presence of complex DNA lesions. EXO1/BLM exonucleases may readily promote resection due to the structure of the DSB terminal, to which Ku cannot bind. It has not been fully investigated whether all the resected DSB ends are repaired by a precise HR pathway or other error prone pathways, e.g. alt-NHEJ, SSA or other pathways.

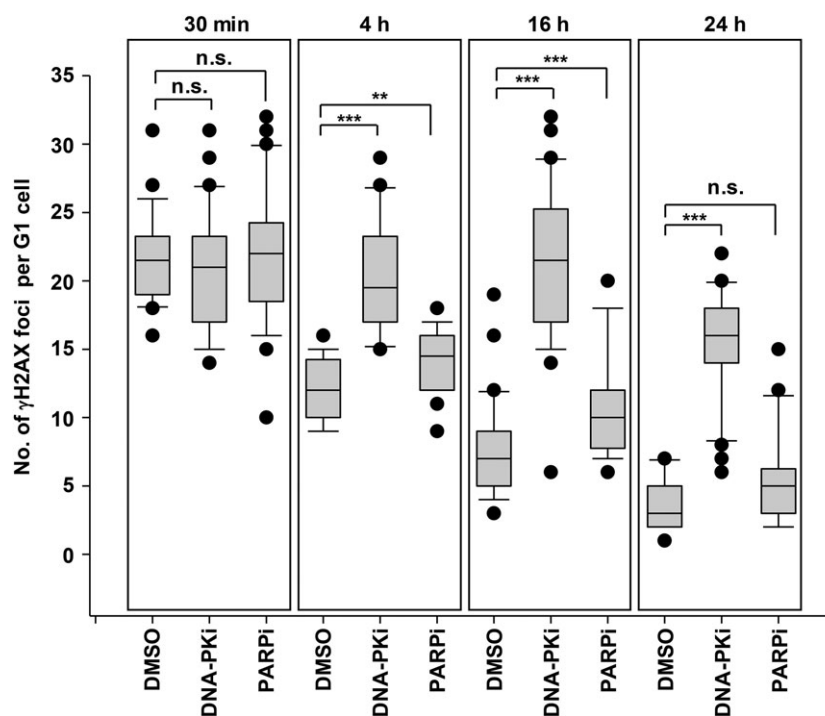


**Fig. 5.** c-NHEJ is the major DSB repair pathway in G1 phase following high-LET heavy-ion irradiation. Olaparib (10  $\mu$ M KU-0059436) was added 30 min before IR. 1BR hTERT, human normal fibroblasts, were irradiated with 3 Gy carbon ions (290 MeV/n, Mono, 70 keV/ $\mu$ m), and cells were fixed at indicated time points. G1 cells were identified as CENPF-/EdU-(39). A box plot of a single experiment is shown. Similar results were obtained in two independent experiments. \* $P < 0.05$ , \*\* $P < 0.01$ , \*\*\* $P < 0.001$ .

current model proposes that if rapid NHEJ does not ensue in a time-dependent manner, DSBs initiate resection and undergo HR in G2 cells [31]. In fact, the magnitude of the damage complexity correlates with the DSB repair kinetics; therefore, it has been proposed that the delay of NHEJ in G2 increases the fraction undergoing HR after high-LET particle irradiation [31] (see discussion in Fig. 4). Several groups have reported higher resection following heavy-ion irradiation compared with that following X-rays or  $\gamma$ -irradiation [31, 32, 38]. However, it has not been determined why DSBs preferentially undergo resection following heavy-ion irradiation. One possibility is that SSBs near a DSB in a complex DNA lesion trigger the initiation of DSB end resection (Fig. 4B). At DSB ends, following X-ray or  $\gamma$ -irradiation exposure, DSB end resection is initiated by CtIP- and MRE11-dependent incision, which forms nicks on the 5'-3' strand [44–47]. Since the Ku70/80 complex blocks DSB ends following X-ray or  $\gamma$ -irradiation, the step of nick formation is essential for initiating 5'-3' resection by EXO1/DNA2/BLM. Thus, if SSBs are formed together with a DSB, these may initiate EXO1-dependent resection. Base damage may also promote the initiation of resection, because SSBs can be formed by apurinic/aprimidinic (AP) endonuclease activity during base excision repair [48, 49]. Therefore, the generation of either SSBs or base damage around a DSB may be a trigger for heavy-ion-specific DSB end resection. As an alternative possibility for how heavy-ion irradiation leads to high levels of resection, the status of the Ku70/80 complex could be considered. The Ku70/80 complex may not be able to bind DSBs induced by heavy-ion irradiation because multiple proteins are

recruited at complex DNA lesions prior to the recruitment of the Ku70/80 complex, or rapid resection leads to the formation of single-stranded DNA (ssDNA), followed by recruitment of RPA on ssDNA. However, since the Ku70/80 complex shows strong binding activity to DSB ends and protects DSB ends, and is highly abundant [50, 51], the Ku70/80 complex is unlikely outcompeted at DSB ends. The identification of such complex DNA lesions and repair pathway will uncover the molecular mechanisms underlying DSB repair and pathway use, which will help increase our understanding of the strong cell-killing effect observed in heavy-ion therapy, because chromosomal rearrangements are often generated via resection-mediated rejoining. Furthermore, we believe it is important to elucidate the pathway for cell death in heavy-ion-irradiated cells because it is still largely unclear how heavy-ion-irradiated cells undergo cell death or persistent growth arrest, e.g. SLGA. Although cellular fate after IR has a high likelihood of being dependent on the IR dose or cell line, it is important to investigate the precise processes from chromosomal rearrangements to cell death, including cell death mode, e.g. apoptosis, mitotic catastrophe, or SLGA, in each case and elucidate the difference between photon and high-LET heavy-ion irradiation. Considering the cause of cell death in cancer cells in heavy-ion therapy, we prefer the idea that chromosomal rearrangement is a major factor leading to cancer cell death, particularly in p53-mutated cancer cells. To support this notion, we previously demonstrated that p53-negative cancer cells frequently undergo cell death showing the features of mitotic catastrophe [52]. Because mitotic catastrophe is caused by chromosome mis-segregation



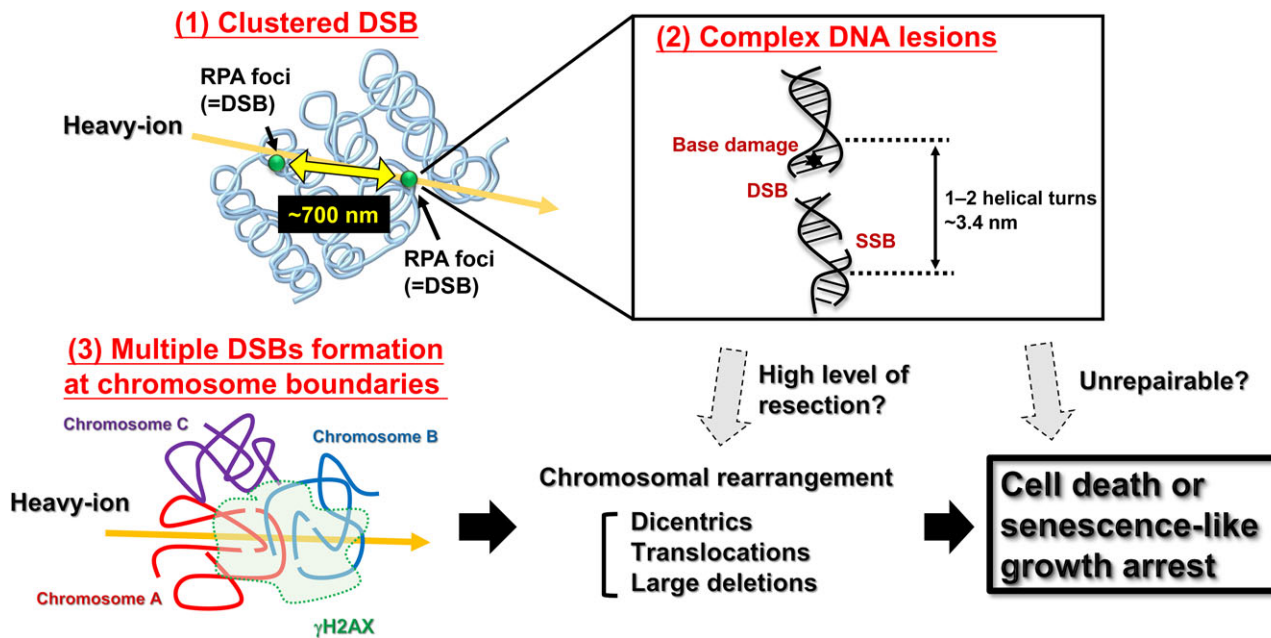


Fig. 6. Hallmarks of DNA damage following heavy-ion irradiation. Schematic diagram for how heavy-ion irradiation induced complex DNA lesions and chromosome rearrangements led to cell death or senescence-like growth arrest (SLGA). (1) High-LET heavy-ion radiation causes clustered DSBs along the particle track. (2) In addition, high-LET heavy-ion radiation causes complex DNA lesions, which contain DSBs, SSBs and/or base damage within 1–2 helical turns. These types of damage are rarely observed in X-ray-irradiated cells. (3) We identified the formation of clustered DSBs at the chromosome boundaries along the particle track. The formation of clustered DSBs at the chromosome boundaries can be a critical risk for chromosomal rearrangements such as dicentrics, translocations and large deletions. The two major types of deletion (i.e. interstitial deletion and terminal deletion) are induced by IR. Small chromosome fragments are produced following interstitial deletion if multiple DSBs in close proximity occur in a single chromosome. Because these fragments can be recognized as DSBs and are not readily repaired, the persistent fragments activate cell cycle checkpoint arrest, apoptosis, or SLGA. High-LET radiation produces such interstitial deletion-derived fragments more frequently than X-ray irradiations, because clustered DSBs are generated along the particle track. In general, chromosome rearrangements including dicentrics, translocations and large deletions induce cell death or SLGA in the first mitosis or after the mitosis. In contrast, interstitial deletions, followed by the formation of fragments, cause cell death and/or SLGA in non-dividing cells. In future work, it will be important to elucidate the impact of complex DNA lesions on cell fate, i.e. whether a high level of resection or the existence of unrepairable damage due to complex DNA lesions affects chromosome rearrangement, cell death and SLGA.

during mitosis or by critical DNA fragmentation in the progression of the next cell cycle phase following the first mitosis, the idea is supported that the scenario of clustered DSBs at a chromosome boundary proceeding to chromosomal rearrangement is likely one of the major pathways leading to cell death through mitotic catastrophe after high-LET particle therapy.

Taken together, the understanding of the molecular mechanisms underlying DSB repair and the repair products, including mis-repair, will help in the development of protection from cancer after exposure to environmental radiation sources and will also contribute to improving heavy-ion radiotherapy.

#### ACKNOWLEDGEMENTS

We thank Yoshimi Omi, Yoko Hayashi, Akiko Shibata, Yuka Hirota and Shiho Nakanishi for assistance with lab work. This work was done as a part of Research Project with Heavy Ions at Gunma University Heavy Ion Medical Center (GHMC). We would like to

thank the GHMC engineering staff for providing support for our heavy-ion experiments.

#### CONFLICT OF INTEREST

The founding sponsors had no role in the design of the study; in the collection, analyses, or interpretation of data; in the writing of the manuscript; or in the decision to publish the results.

#### FUNDING

This work was supported by Grants-in-Aid from the Japan Society for the Promotion of Science for KAKENHI (JP26701005 and JP17H04713 to A.S.), the Takeda Science Foundation and the Uehara Memorial Foundation. This work was supported by the Program of the network-type Joint Usage/Research Center for Radiation Disaster Medical Science of Hiroshima University, Nagasaki University, and Fukushima Medical University. This work was also supported by Grants-in-Aid from the Ministry of

Education, Culture, Sports, Science and Technology of Japan for programs for Leading Graduate Schools, Cultivating Global Leaders in Heavy Ion Therapeutics and Engineering.

## REFERENCES

- Ritter S, Durante M. Heavy-ion induced chromosomal aberrations: a review. *Mutat Res* 2010;701:38–46.
- Durante M, Cucinotta FA. Heavy ion carcinogenesis and human space exploration. *Nat Rev Cancer* 2008;8:465–72.
- Durante M, Orecchia R, Loeffler JS. Charged-particle therapy in cancer: clinical uses and future perspectives. *Nat Rev Clin Oncol* 2017;14:483–95.
- Veldeman L, Madani I, Hulstaert F et al. Evidence behind use of intensity-modulated radiotherapy: a systematic review of comparative clinical studies. *Lancet Oncol* 2008;9:367–75.
- Loeffler JS, Durante M. Charged particle therapy—optimization, challenges and future directions. *Nat Rev Clin Oncol* 2013;10:411–24.
- Nakano T, Mitsusada Y, Salem AM et al. Induction of DNA-protein cross-links by ionizing radiation and their elimination from the genome. *Mutat Res* 2015;771:45–50.
- Shibata A, Jeggo PA. DNA double-strand break repair in a cellular context. *Clin Oncol (R Coll Radiol)* 2014;26:243–9.
- Yatagai F, Kurobe T, Nohmi T et al. Heavy-ion-induced mutations in the *gpt* delta transgenic mouse: effect of *p53* gene knockout. *Environ Mol Mutagen* 2002;40:216–25.
- Masumura K, Kuniya K, Kurobe T et al. Heavy-ion-induced mutations in the *gpt* delta transgenic mouse: comparison of mutation spectra induced by heavy-ion, X-ray, and gamma-ray radiation. *Environ Mol Mutagen* 2002;40:207–15.
- Ushigome T, Shikazono N, Fujii K et al. Yield of single- and double-strand breaks and nucleobase lesions in fully hydrated plasmid DNA films irradiated with high-LET charged particles. *Radiat Res* 2012;177:614–27.
- Friedland W, Schmitt E, Kundrat P et al. Comprehensive track-structure based evaluation of DNA damage by light ions from radiotherapy-relevant energies down to stopping. *Sci Rep* 2017;7:45161.
- Hagiwara Y, Niimi A, Isono M et al. 3D-structured illumination microscopy reveals clustered DNA double-strand break formation in widespread  $\gamma$ H2AX foci after high LET heavy-ion particle radiation. *Oncotarget* 2017;8:109370–81.
- Soutoglou E, Dorn JF, Sengupta K et al. Positional stability of single double-strand breaks in mammalian cells. *Nat Cell Biol* 2007;9:675–82.
- Roukos V, Voss TC, Schmidt CK et al. Spatial dynamics of chromosome translocations in living cells. *Science* 2013;341:660–4.
- Roukos V, Misteli T. The biogenesis of chromosome translocations. *Nat Cell Biol* 2014;16:293–300.
- Desai N, Davis E, O'Neill P et al. Immunofluorescence detection of clustered  $\gamma$ -H2AX foci induced by HZE-particle radiation. *Radiat Res* 2005;164:518–22.
- Leatherbarrow EL, Harper JV, Cucinotta FA et al. Induction and quantification of  $\gamma$ -H2AX foci following low and high LET-irradiation. *Int J Radiat Biol* 2006;82:111–8.
- Nakajima NI, Brunton H, Watanabe R et al. Visualisation of  $\gamma$ H2AX foci caused by heavy ion particle traversal; distinction between core track versus non-track damage. *PLoS ONE* 2013;8:e70107.
- Oike T, Niimi A, Okonogi N et al. Visualization of complex DNA double-strand breaks in a tumor treated with carbon ion radiotherapy. *Sci Rep* 2016;6:22275.
- Reindl J, Girst S, Walsh DW et al. Chromatin organization revealed by nanostructure of irradiation induced  $\gamma$ H2AX, 53BP1 and Rad51 foci. *Sci Rep* 2017;7:40616.
- Lorat Y, Brunner CU, Schanz S et al. Nanoscale analysis of clustered DNA damage after high-LET irradiation by quantitative electron microscopy—the heavy burden to repair. *DNA Repair* 2015;28:93–106.
- Lorat Y, Timm S, Jakob B et al. Clustered double-strand breaks in heterochromatin perturb DNA repair after high linear energy transfer irradiation. *Radiother Oncol* 2016;121:154–61.
- Schermelleh L, Heintzmann R, Leonhardt H. A guide to super-resolution fluorescence microscopy. *J Cell Biol* 2010;190:165–75.
- Branco MR, Pombo A. Intermingling of chromosome territories in interphase suggests role in translocations and transcription-dependent associations. *PLoS Biol* 2006;4:e138.
- Meaburn KJ, Misteli T. Cell biology: chromosome territories. *Nature* 2007;445:379–781.
- Misteli T, Soutoglou E. The emerging role of nuclear architecture in DNA repair and genome maintenance. *Nat Rev Mol Cell Biol* 2009;10:243–54.
- Bunting SF, Nussenzweig A. End-joining, translocations and cancer. *Nat Rev Cancer* 2013;13:443–54.
- Yamauchi M, Shibata A, Suzuki K et al. Regulation of pairing between broken DNA-containing chromatin regions by Ku80, DNA-PKcs, ATM, and 53BP1. *Sci Rep* 2017;7:41812.
- Niimi A, Yamauchi M, Limsirichaikul S et al. Identification of DNA double strand breaks at chromosome boundaries along the track of particle irradiation. *Genes Chromosomes Cancer* 2016;55:650–60.
- Beucher A, Birraux J, Tchouandong L et al. ATM and Artemis promote homologous recombination of radiation-induced DNA double-strand breaks in G2. *EMBO J* 2009;28:3413–27.
- Shibata A, Conrad S, Birraux J et al. Factors determining DNA double-strand break repair pathway choice in G2 phase. *EMBO J* 2011;30:1079–92.
- Yajima H, Fujisawa H, Nakajima NI et al. The complexity of DNA double strand breaks is a critical factor enhancing end-resection. *DNA Repair* 2013;12:936–46.
- Lee R, Nasonova E, Hartel C et al. Chromosome aberration measurements in mitotic and G2-PCC lymphocytes at the standard sampling time of 48 h underestimate the effectiveness of high-LET particles. *Radiat Environ Biophys* 2011;50:371–81.
- Wu W, Wang M, Wu W et al. Repair of radiation induced DNA double strand breaks by backup NHEJ is enhanced in G2. *DNA Repair* 2008;7:329–38.
- Wang M, Wu W, Wu W et al. PARP-1 and Ku compete for repair of DNA double strand breaks by distinct NHEJ pathways. *Nucleic Acids Res* 2006;34:6170–82.
- Ceccaldi R, Rondinelli B, D'Andrea AD. Repair pathway choices and consequences at the double-strand break. *Trends Cell Biol* 2016;26:52–64.

37. Deckbar D, Birraux J, Krempler A et al. Chromosome breakage after G2 checkpoint release. *J Cell Biol* 2007;176:749–55.
38. Averbeck NB, Ringel O, Herrlitz M et al. DNA end resection is needed for the repair of complex lesions in G1-phase human cells. *Cell Cycle* 2014;13:2509–16.
39. Biehs R, Steinlage M, Barton O et al. DNA double-strand break resection occurs during non-homologous end joining in G1 but is distinct from resection during homologous recombination. *Mol Cell* 2017;65:671–84 e5.
40. Oike T, Sato H, Noda SE et al. Translational research to improve the efficacy of carbon ion radiotherapy: experience of Gunma University. *Front Oncol* 2016;6:139.
41. Kamada T, Tsujii H, Blakely EA et al. Carbon ion radiotherapy in Japan: an assessment of 20 years of clinical experience. *Lancet Oncol* 2015;16:e93–100.
42. Chan N, Pires IM, Bencokova Z et al. Contextual synthetic lethality of cancer cell kill based on the tumor microenvironment. *Cancer Res* 2010;70:8045–54.
43. Deckbar D, Stiff T, Koch B et al. The limitations of the G1-S checkpoint. *Cancer Res* 2010;70:4412–21.
44. Sartori AA, Lukas C, Coates J et al. Human CtIP promotes DNA end resection. *Nature* 2007;450:509–14.
45. Shibata A, Moiani D, Arvai AS et al. DNA double-strand break repair pathway choice is directed by distinct MRE11 nuclease activities. *Mol Cell* 2014;53:7–18.
46. Nimonkar AV, Genschel J, Kinoshita E et al. BLM-DNA2-RPA-MRN and EXO1-BLM-RPA-MRN constitute two DNA end resection machineries for human DNA break repair. *Genes Dev* 2011;25:350–62.
47. Makharashvili N, Tubbs AT, Yang SH et al. Catalytic and non-catalytic roles of the CtIP endonuclease in double-strand break end resection. *Mol Cell* 2014;54:1022–33.
48. Mourgues S, Lomax ME, O'Neill P. Base excision repair processing of abasic site/single-strand break lesions within clustered damage sites associated with XRCC1 deficiency. *Nucleic Acids Res* 2007;35:7676–87.
49. Lomax ME, Cunniffe S, O'Neill P. Efficiency of repair of an abasic site within DNA clustered damage sites by mammalian cell nuclear extracts. *Biochemistry* 2004;43:11017–26.
50. Falzon M, Fewell JW, Kuff EL. EBP-80, a transcription factor closely resembling the human autoantigen Ku, recognizes single- to double-strand transitions in DNA. *J Biol Chem* 1993;268:10546–52.
51. Liang F, Jasin M. Ku80-deficient cells exhibit excess degradation of extrachromosomal DNA. *J Biol Chem* 1996;271:14405–11.
52. Amornwichee N, Oike T, Shibata A et al. Carbon-ion beam irradiation kills X-ray-resistant p53-null cancer cells by inducing mitotic catastrophe. *PLoS ONE* 2014;9:e115121.
53. Shibata A. Regulation of repair pathway choice at two-ended DNA double-strand breaks. *Mutat Res* 2017;803–805:51–5.